The Egyptian Journal of Hospital Medicine (January 2018) Vol. 70 (2), Page 312-324

Role of MRI in Characterization of Benign Hepatic Focal Lesions

Mohamed Abdul Aziz Ali*, Ahmed Mohamed Hussein*, Rawnaq Ahmed Tuayen**
*Radiodiagnosis Department, Faculty of Medicine, Ain Shams University, ** Basrah University

ABSTRACT

Background: nowadays, magnetic resonance plays a key role in management of liver lesions, using a radiation-free technique and a safe contrast agent profile. The heightened soft-tissue resolution and sensitivity to intravenous contrast agents provided by magnetic resonance imaging (MRI) makes it an invaluable problem-solving tool for fully characterizing focal liver lesions (FLL). Diffusion-weighted imaging (DWI) sequences have been shown to be an emerging contributor for liver MRI and are being incorporated in most abdominal MR protocols**.**

Aims: To determine the role of MRI in characterization of benign hepatic focal lesions.

Patients and methods: This study included 30 patients (11 M, 19 F with mean age of 47.7 years) with benign hepatic focal lesions. They were simple cyst (n =6), hemangioma (n = 11), abscess (n = 4), adenoma (n = 2), focal nodular hyperplasia (n = 3), Hydatid cyst (n=1) and regenerative nodules (n = 3). They underwent routine MR imaging and diffusion MR weighted imaging using 1.5 tesla MR unit (Philips Achieva). Diffusion MR imaging was done using spin echo type of single shot echo planar imaging (EPI) with b value of 0, &800 mm2/sec. The apparent diffusion coefficient (ADC) map was reconstructed and ADC value was measured. The mean ADC values correlated with histopathological results as well as follow-up imaging results. **Results:** The mean ADC values were significantly different within benign hepatic focal lesions ($P < 0.001$). There was highly statically significant relation between cyst and hemangioma (p-value < 0.001), cyst and abscess (p-value <0.001), hemngioma and abscess (p-value < 0.001), while there was no statically significance relation between adenoma and focal nodular hyperplasia (p-value < 0.74), adenoma and regenerative nodules (p-value < 0.67) and focal nodular hyperplasia and regenerative nodules (p-value < 0.41). **Conclusions:** benign liver lesions are frequently encountered in clinical practice and their characterization may be sometimes difficult. The problem of lesion characterization is mainly crucial and may influence therapeutic decisions and patient's management. The role of imaging is therefore a mainstay and MRI, with its multi parametric potentialities, is a highly accurate method for lesion detection and characterization. Nevertheless, benign lesions may be sometimes "non-typic" in their cellular content and vascular behavior and lesions biopsy can be necessary for definitive characterization.

Keywords: MRI, DWI, hepatic focal lesions.

INTRODUCTION

Nowadays, magnetic resonance plays a key role in management of liver lesions, using a radiation-free technique and a safe contrast agent profile [(1)].The heightened soft-tissue resolution and sensitivity to intravenous contrast agents provided by magnetic resonance imaging (MRI) makes it an invaluable problem-solving tool for fully characterizing focal liver lesions (FLL) [(2)].The majority of FLL arising in non-cirrhotic liver are benign, even in patients with known extra-hepatic malignancy. Cysts, hemangiomas, focal nodular hyperplasias (FNH), and hepatocellular adenomas (HCA) are the most commonly encountered benign lesions [(3)]**.** A tremendous development of new imaging techniques has taken place during these last years. Maximizing accuracy of imaging in the context of FLL is paramount in avoiding unnecessary biopsies, which may result in post-procedural complications up to 6.4%, and mortality up to 0.1% [(4)]. Definitive characterization by magnetic resonance (MR) imaging may alleviate patient anxiety, drastically alter management in someone and help avoid unnecessary biopsy or costly follow-up imaging. MR imaging offers important advantages over computed tomography (CT), such as the lack of ionizing radiation and improved soft tissue contrast [(5)]. MRI can be used as the primary imaging examination for patients who cannot receive iodinated IV contrast material and patients in whom the liver is the only organ of concern. MRI is useful as a problem solving technique when other imaging study showed equivocal findings [(6)].

The American College of Radiology Appropriateness Criteria assigned the highest rating to MR imaging with and without contrast for characterization of indeterminate liver lesions, regardless of whether the patient is otherwise healthy, has liver disease, or has a known extra hepatic malignancy [(7)]**.** With the current state of the art technology, magnets of 1.5 Tesla (T) and 3T field strength are considered the standard of reference in providing high-quality and consistent MR images. Giant advances in MRI have been achieved in the last decade in regards to each of the following: hardware (high-performance

Received: 10/10/2017
Accepted: 20/10/2017
DOI: 10.12816/0043097

gradient coils and phased-array surface coils), software (new sequence design and new parallel imaging technology and acceleration techniques) and contrast agents (hepatocyte-specific agents) have made a major impact on imaging of the liver [(8)]. The state of the art MRI protocols rely on a combination of fat-suppressed and non-fat-suppressed T2-weighted images (T2-WI), in- and opposed-phase (IP/OP) T1-WI and dynamic pre- and post-contrast fat-suppressed T1-WI [(9)]. Detection and characterization of focal hepatic lesions continues to be a challenge. Magnetic resonance (MR) imaging plays an important role in evaluation of a wide range of benign and malignant focal hepatic lesions. The use of three-dimensional (3D) gradient-recalled-echo (GRE) sequences such as volumetric interpolated breath-hold examination (VIBE) has improved MR imaging by providing dynamic contrast material–enhanced thin-section images with fat saturation and a high signal-to-noise ratio [(10)].

Contrast-enhanced 3D GRE MR imaging demonstrated characteristic enhancement patterns that can be helpful in the diagnosis of various focal hepatic lesions. These enhancement patterns are seen during specific phases of imaging and included arterial phase enhancement, delayed phase enhancement, peripheral washout, ring enhancement, nodule-within-a-nodule enhancement, true central scar, pseudocentral scar and pseudo-capsule [(11)].

Diffusion-weighted imaging (DWI) sequences have been shown to be an emerging contributor for liver MRI and are being incorporated in most abdominal MR protocols [(12)].

The underlying principle is that different biologic tissues exhibit varying levels of restricted water diffusion, dependent on such factors as tissue cellularity and cell membrane integrity [(13)].

AIM OF THE WORK

This study aimed to detect the role of MRI in characterization of benign hepatic focal lesions.

PATIENTS and METHODS:

Study Population:

This study was performed between March 2016 and April 2017 in Radiology Department, Faculty of Medicine, Ain Shams University Hospital, a total of thirty cases with suspicion of focal liver lesions on the basis of US and/or CT were included.

Inclusion Criteria

Patient known to have focal liver lesion detected by US &/or MSCT.

Exclusion Criteria

1. **Patients with general contraindications to MRI:**
   - Ferromagnetic prosthesis (aneurysmal clip, surgical clips) or foreign bodies.
   - Cardiac pacemaker.
   - Claustrophobia or with unstable clinical status.
2. **Contraindications to contrast media administration:**
   - History of prior allergic reaction to gadolinium chelates.
   - Relative contraindication to gadolinium chelates (such as pregnancy).
   - Impaired renal function, which was defined as serum creatinine level > 200 μmol/L.
3. **Patients with bad general condition (e.g. tense ascites) and/or unable to hold breath.**

The patients were subjected to the following:

1. Full clinical assessment including; recording of age, sex and clinical presentation.
2. Informed consent was taken from all the patients after explaining the entire procedure, its benefits and risks.
3. Laboratory investigations, if clinically indicated.
4. Abdominal MRI (non contrast enhanced, dynamic post contrast and diffusion weighted MRI).

MR IMAGING

MR imaging was performed on high field system (1.5 Tesla- Philips Achieva) using a phased array coil (SENSE XL Torso 16 element) to cover the whole liver.

Instructions and preparation of the patients:

1) Reassurance of the patients, simple explanation of the procedures & instructing the patients to keep motionless & breathe calmly during the examination time.
2) On the examination table a tight abdominal compression was applied to the upper abdomen during exhalation to reduce the respiratory motion artifacts.
3) A venous catheter was placed in a peripheral vein (ante-cubital vein in most cases) being through a long connecting tube to automatic injector to allow easy injection.

MR USED PROTOCOL

A. Pre-contrast imaging:

- **Axial T1 weighted (T1W) images:** repetition time (TR)=4msec, echo time (TE)=2msec, matrix 192x192, slice thickness 10mm, slice gap 1-2 mm, and scan time = 15.3 sec.
- **Axial T2 weighted (T2W-TSE SENSE):** TR 500-510 msec, TE=90-100 msec, matrix 384

x 384 with a slice thickness 10 mm, slice gap 2mm, FA= 90 degrees &Scan time = 2-5 min.

- **Axial in phase and out phase gradient echo sequence (dual-FFE-BH-SENSE) axial images:** TR= 170msec, TE=4.6msec for in phase and 2.3msec for out phase, matrix 384x384 with slice thickness 10mm, slice gap 2 mm & flip angle = 80, Scan time = 1.20 sec.
- **Axial T2 SPAIR (Spectral Attenuated Inversion Recovery) fat suppression sequence:** TR 412 – 418 msec, TE=80msec, matrix 384 x 384 with a slice thickness 10 mm, slice gap 2mm, scan time = 1.12 min.
- **Axial heavy T2 weighted images**: TR=737msec, TE=300msec, matrix 400 x 400 with a field of view: 381, slice thickness 10 mm, slice gap 2 mm.
- **Coronal T2W-TSE SENSE:** TR =500msec, TE= 100 msec, matrix 528x528 with a field of view: 365, slice thickness 3mm, slice gap 0mm and flip angle of 10 degrees, scan time =1.36 min.
- **Coronal Survey BFFE**: TR=2.85, TE=1.43, Matrix=256x256, slice thickness=15mm, slice gap=3mm and Flip Angle=60º: Scan time = 57 sec.

B. Diffusion study

Diffusion-weighted imaging was performed using respiratory triggered protocol at *b* value 0 and 800, with the single shot echo-planar imaging (EPI) technique in axial plane, Parameters were as follows:

Repetition time (TR) = 1852 ms, echo time (TE) = 70 ms, number of excitations (NEX) = 3, matrix 150x236 with a field of view as small as possible, slice thickness 4 mm, slice gap 0.5 mm, scan time 5 min. Qualitative assessment at different b values and quantitative assessment by measuring ADC values were done. ADC maps were reconstructed on the workstation. Two b values (0, and 800 mm^2/s) were used for ADC calculation. The ADC value of each focal liver lesion (FLL) was calculated within a region of interest (ROI) placed in the center of the assessed lesion, covering more than 50% of its surface, in cases of scar, necrotic tissue, measurements were taken only in the solid part, trying to avoid inclusion within the ROI.

Each lesion was individually analyzed in cases with multiple FLLs. Mean ADC measurement was calculated for each hepatic pathology.

C. Dynamic study:

Dynamic study was performed after bolus injection of 0.1mmol/kg body weight of Gd-DTPA at a rate of 2ml/s, flushed with 20ml of sterile 0.9% saline solution in the antecubital vein. Dynamic imaging using THRIVE (T1 High Resolution Isotropic Volume Examination) technique which is 3D GRE with fat suppression (SPAIR) performed before and after contrast administration in arterial, porto-venous as well delayed phase. The patient was asked to hold breath at end expiration.

- **Coronal 2D BOLUS TRACK:** TR =4mses, TE=0.79-1.82 msec, matrix 256x256 with a field of view: 365, slice thickness 3mm, slice gap 0mm and flip angle of 10 degrees, scan time = 2.34 min.
- **eThrive Dynamic Sense**: TR =3.77-3.85ms, TE=1.79-1.82 msec, matrix 192x192 with a field of view: 365, slice thickness 3mm, slice gap 0mm and flip angle of 10 degrees, scan time = 1.01 min.

Image analysis

The following data were recorded for each benign hepatic focal lesion: site, size, morphology, signal intensity of all used sequences (T1WI, T2WI FSE, STIR, dynamic contrast material–enhanced, DWI and ADC map).

Our standard of reference was based on the histopathological findings in addition to MRI finding for solid benign focal lesions and abscess, other benign lesions (hepatic cysts and hemangiomas) of typical MRI findings, no histopathological confirmation was done, just follow-up.

Statistical analysis

Data were analyzed using Statistical Program for Social Science (SPSS) version 24.0. Quantitative data were expressed as mean ± standard deviation (SD). Qualitative data were expressed as frequency and percentage.

The following tests were done:

- A one-way analysis of variance (ANOVA) when comparing between more than two means.
- Chi-square (X^2) test of significance was used in order to compare proportions between two qualitative parameters.
- The confidence interval was set to 95% and the margin of error accepted was set to 5%. So, the p-value was considered significant as the following:
- Probability (P-value)

– P-value <0.05 was considered significant.
– P-value <0.001 was considered as highly significant.
– P-value >0.05 was considered insignificant.

The study was done after approval of ethical board of Ain Shams university.

RESULTS

The studied group was consisted of 30 patients and the results were analyzed as follow*:*

Patient's characteristics:

Table 4: age wise distribution of benign hepatic focal lesions

Age (years)	No. of patients	Percentage
≤50 years	18	60
>50 years	12	40
Total	**30**	**100**
Mean	**47.7**	

In the present study maximum percentage of patients were in age **≤50 years** (60%). Mean age of patients in the study was **47.7** years.

Table 5: sex wise distribution of the benign hepatic focal lesions

Sex	No. of patients	Percentage
Female	19	63.3
Male	11	36.7
Total	**30**	**100**

In the present study there was female preponderance (63.3%), when compared to females (36.7%).

Table 6: distribution of patient according to multiplicity of benign hepatic focal lesions.

Type of lesion	No. of patients	Percentage
Single	22	73.3
Multiple	8	26.7
Total	30	100

In the present study, 76.7% of patients had single hepatic focal lesions.

Table 7: distribution of patients according to diagnosis

MRI diagnosis	No. of patients	Percentage
Hemangioma	11	36.7
Simple cyst	6	20
Abscess	4	13.3
Focal nodular hyperplasia	3	10
Regenerative nodule	3	10
Adenoma	2	6.7
Hydatid cyst	1	3.3
Total	**30**	**100**

In the present study, most common lesion was hemangioma (36.7%) and simple cysts were 20%.

MRI characteristics

The behavior of benign hepatic focal lesions in non-contrast enhanced, dynamic enhanced and DWI –MRI were as follow:

On non-contrast enhanced MRI

In T1WI, the lesions showed hypointense signal intensity were hemangiona (48.6%), simple hepatic cyst (28.6%), abscess (11.4%), hydatid cyst (2.9%), adenoma (2.9%), focal nodular hyperplasia (5.7%).

Lesions elicited hyper intense signal intensity were regenerative nodules, while lesions appeared with iso intense signal intensity were adenoma (3.3%), focal nodular hyperplasia (50%), regenerative nodule (50%) **(Table 8).**

Table 8: variable T1WI signal intensities of different MRI lesions

T1WI		MRI Diagnosis							Chi-square	
		Abscess	Adenoma	Focal nodular hyperplasia	Hemangioma	Hydatid Cyst	Regenerative nodule	Simple cyst	X^2	p-value
Hyperintense	No.	0	0	0	0	0	5	0	58.1	<0.001
	%	0.0%	0.0%	0.0%	0.0%	0.0%	100.0%	0.0%		
Hypointense	No.	4	1	2	17	1	0	10		
	%	11.4%	2.9%	5.7%	48.6%	2.9%	0.0%	28.6%		
Isointense	No.	0	1	1	0	0	0	0		
	%	0.0%	50.0%	50.0%	0.0%	0.0%	0.0%	0.0%		

This table showed highly statistically significant relation between benign focal liver lesions and T1 signal intensity. In T2WI, the lesions showed hyper-intense signal intensity was hemangiona (47.2%) simple hepatic cyst (27.8%), abscess (11.1%), adenoma (5.6%), focal nodular hyperplasia (5.6%), hydatid cyst (2.8%). Lesions appeared with hypointense signal intensity were regenerative nodules (100%), While lesions appeared with isointense signal intensity focal nodular hyperplasia (100%) **(Table 9).**

Table 9: variable T2WI signal intensities of different MRI lesions

T2WI		MRI Diagnosis							Chi-square	
		Abscess	Adenoma	Focal nodular hyperplasia	Hem-angioma	Hydatid Cyst	Regenerative nodule	Simple cyst	X^2	p-value
Hyperintense	No.	4	2	2	17	1	0	10	55.222	<0.001
	%	11.1%	5.6%	5.6%	47.2%	2.8%	0.0%	27.8 %		
Hypointense	No.	0	0	0	0	0	5	0		
	%	0.0%	0.0%	0.0%	0.0%	0.0%	100.0%	0.0%		
Isointense	No.	0	0	1	0	0	0	0		
	%	0.0%	0.0%	100.0%	0.0%	0.0%	0.0%	0.0%		

This table showed highly statistically significant relation between benign focal liver lesions and T2 signal intensity.

On post contrast dynamic study, the patterns of enhancement were as follows:

1. **Hemangioma:** the enhancement patterns were variable in different phases of dynamic examination, peripheral nodular enhancement is the most common findings in arterial and portal phase as it was seen in 14 out of 17 lesions of hemangioma, while homogenous enhancement (complete fill in) is the commonest finding in delayed phase as it was seen in 15 out of 17 hemangiomas (**Fig. 1).**

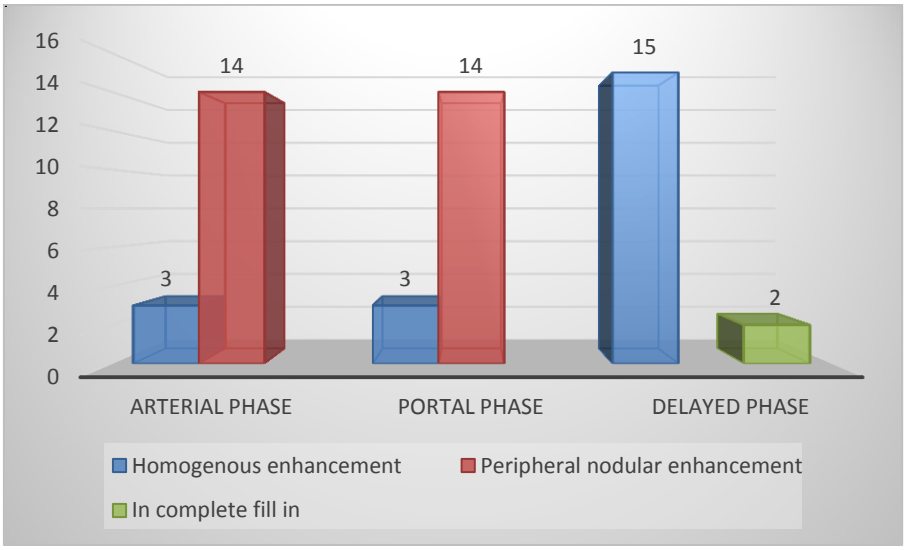

Fig. 1: graph displays different patterns of enhancement of hemangiomas by dynamic MRI

2. **Cysts (simple and hydatid):** in post contrast dynamic study the ten lesions of simple hepatic cyst showed no enhancement in all phases while one lesion of hydatid cyst elicited smooth peripheral enhancement.

3. **Abscess:** in post contrast dynamic study the four lesions showed peripheral ring enhancement in all phases.

4. **Adenoma:** post-contrast dynamic MRI examination the two lesions display heterogeneous enhancement at the arterial & portal phases with delayed washout (**Fig. 2).**

Fig. 2: graph showing pattern of enhancement of hepatic adenoma by dynamic MRI.

5. Focal nodular hyperplasia: post-contrast dynamic MRI examination the three lesions elicited intense arterial phase homogenous enhancement with hypo-enhancing central scar then it became iso-enhanced in both portal and delayed phases, while central scar showed late enhancement in delayed phase.

6. Regenerative nodules: post-contrast dynamic MRI examination the five lesions showed no more different enhancement pattern than adjacent normal liver parenchyma.

On DWI: images analysis was done by:

1. Qualitative assessment on DW imaging:

All cystic lesions and hemangiomas showed facilitated diffusion with significant or near complete loss of signal intensity on increasing b value, and lesions which did not show reduction of signal intensity, showed high signal intensity on ADC map.

Abscesses typically showed restricted diffusion, elicited high signal intensity on DWI and low signal on ADC map.

Solid benign hepatic lesions showed no evidence of restricted diffusion at different b values. On ADC map, there was lower signal intensity compared to surrounding normal liver parenchyma regarding adenoma, FNH while regenerative nodules appeared similar to adjacent hepatic parenchyma.

2. Quantitative (ADC) evaluation:

The mean ADC values were 3.34 ±0.2 x 10^{-3} mm^2/s for simple hepatic cysts, 2.13 ±0.5 x 10^{-3} mm^2/s for hemangiomas, 2.8 x$10^{-3}$$mm^2/s$ for hydatid cyst, 1.46 ±0.01 x$10^{-3}$$mm^2/s$ for focal nodular hyperplasia, 1.35 ±0.07 x$10^{-3}$$mm^2/s$ for adenoma, 1.22 ±0.1 x$10^{-3}$$mm^2/s$ for regenerative nodules, 0.72 x$10^{-3}$$mm^2/s$ for abscess **(Table 10, fig. 3).**

Table 10: mean ADC values of benign liver lesions

ADC value	Mean	Std. Deviation	Range		ANOVA	p-value
Abscess	0.72	0.3	0.32	1.02	28.139	<0.001
Adenoma	1.35	0.07	1.3	1.4		
Focal nodular hyperplasia	1.46	0.01	1.45	1.47		
Hemangioma	2.13	0.5	1.3	2.98		
Hydatid cyst	2.80	0.0	2.8	2.8		
Regenerative nodule	1.22	0.1	1.11	1.31		
Simple cyst	3.34	0.2	3.1	3.52		

In present study there was a highly significant relation between ADC value and benign focal liver lesions.

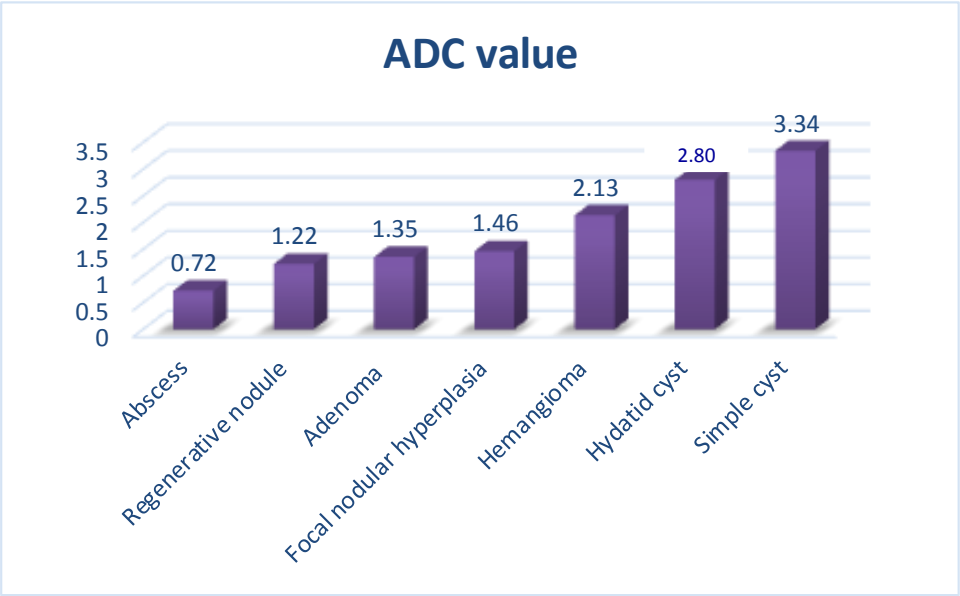

Fig. 3: **ADC value of benign hepatic focal lesions.**

There was a highly statically significant relation between cyst and hemangioma (p-value < 0.001), cyst and abscess (p-value <0.001), hemngioma and abscess (p-value < 0.001), while there was no statically significance relation between adenoma and focal nodular hyperplasia (p-value < 0.74), adenoma and regenerative nodules (p-value < 0.67) and focal nodular hyperplasia and regenerative nodules (p-value < 0.41) (**Table 11).**

Table 11: post hoc ANOVA test for significance between benign focal liver lesions.

MRI diagnosis	Adenoma	Focal nodular hyperplasia	Hemangioma	Regenerative nodule	Cyst
Abscess	0.05	0.01	0.001	0.09	0.001
Adenoma		0.74	0.01	0.67	0.001
Focal nodular hyperplasia			0.01	0.41	0.001
Hemangioma				0.001	0.001
Regenerative nodule					0.001

ILLUSTRATIVE CASES

CASE 1

Clinical history: 37 years old female patient presented with crampy right lower quadrant abdominal pain. U/S was done revealed large isoechoic mass in the right lobe of the liver.

On MRI examination: the liver appears of average size with single large focal lesion about (7.3 x8.3 cm) at hepatic subsegment VIII and V, elicits isointense signal on T1WI (**Fig. 4 A)** (white arrow) with slightly hypo intense central scar (**Fig.4 A)** (white stripped arrow) and isointense signal intensity on T2WI (**Fig.4 B)** (white arrow) with hyper intense central scar **fig.44 B** (white stripped arrow).

Dynamic MRI: the mass showed homogenous intense enhancement on arterial phase **fig.44 C** (white arrow) with hypo enhancing central scar(**Fig.4 C)** (black stripped arrow). On a portal and delayed phase, the mass fade and become isointense relative to the adjacent liver **fig.4 C, D** (white arrow) with delayed enhancement of central scar (**Fig.4 C)** (black stripped arrow).

DWI: the mass showed slight increase in signal intensity with increase b values(**Fig.4 F,G)** (white arrow) and low signal on ADC map (**Fig.4 H)** (white arrow).

ADC Value: 1.47 x $10^{-3}$$mm^2$/sec.

MRI diagnosis: focal nodular hyperplasia.

Histopathological diagnosis: focal nodular hyperplasia.

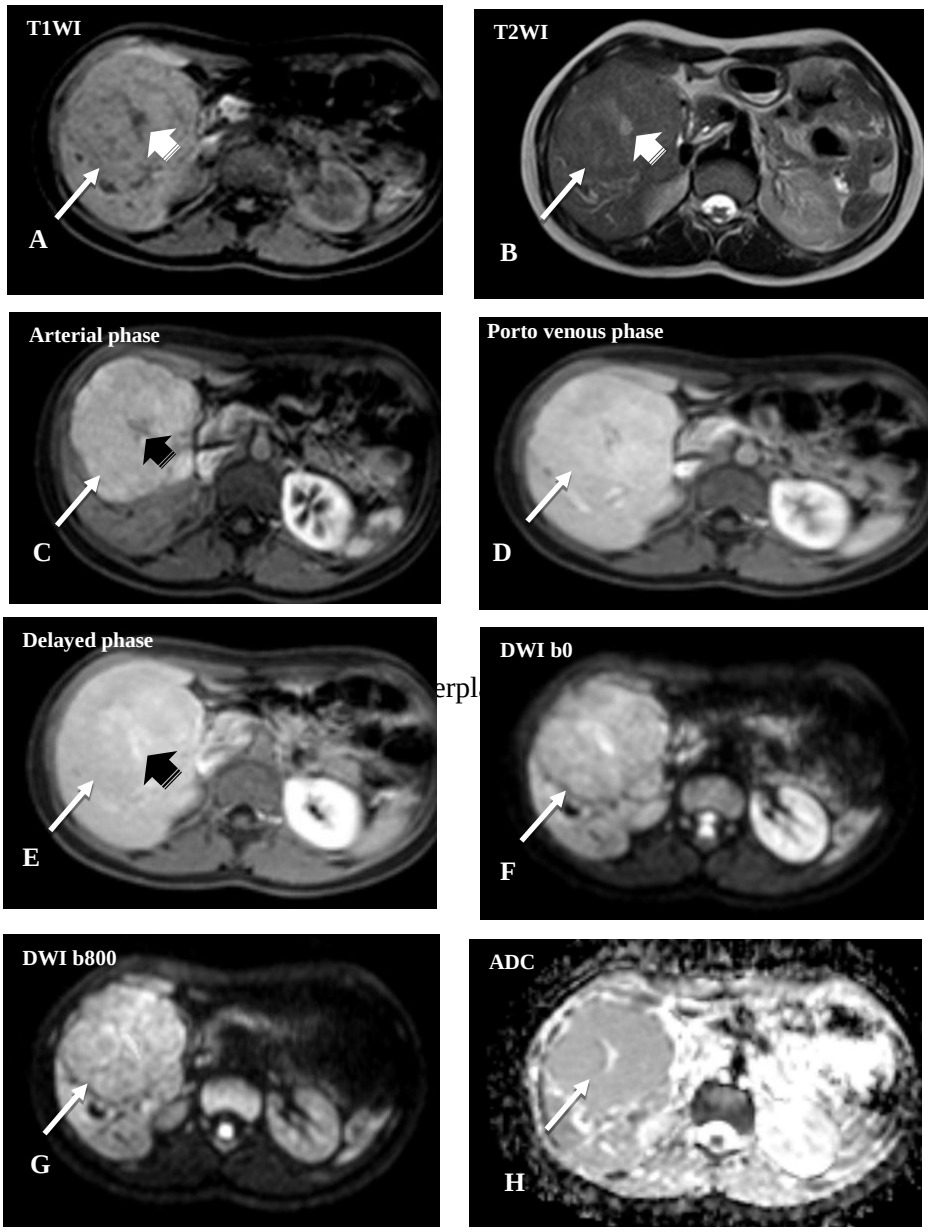
T1WI
A
T2WI
B
Arterial phase
C
Porto venous phase
D
Delayed phase
E
DWI b0
F
DWI b800
G
ADC
H

CASE 2

Clinical history: 53 years old female patient presented with history of right loin pain. U/S was done revealed a hyper echoic single hepatic focal lesion in the right lobe of the liver.

On MRI examination: the right hepatic lobe segment VI was the seat of single lobulated margin focal lesion measuring about (3.5 x 4.8 x 5.8 cm), elicits low T1 and high T2 signals intensities (**Fig. 5 A, B)** (arrows).

Dynamic MRI: the lesion shows peripheral nodular enhancement on arterial phase (**Fig.5 C)** (arrow) and progressive centripetal filling on portal, delayed phases (**Fig.5 D, E)** (arrows).

DWI: the lesion shows decrease in signal intensity with increasing b values (**Fig.5 F, G**)(arrows). While, it showed high signal intensity on ADC map (**Fig. 5 H)** (arrows).

ADC Value: 2.63 x $10^{-3}$$mm^2$/sec

MRI diagnosis: giant hemangioma.

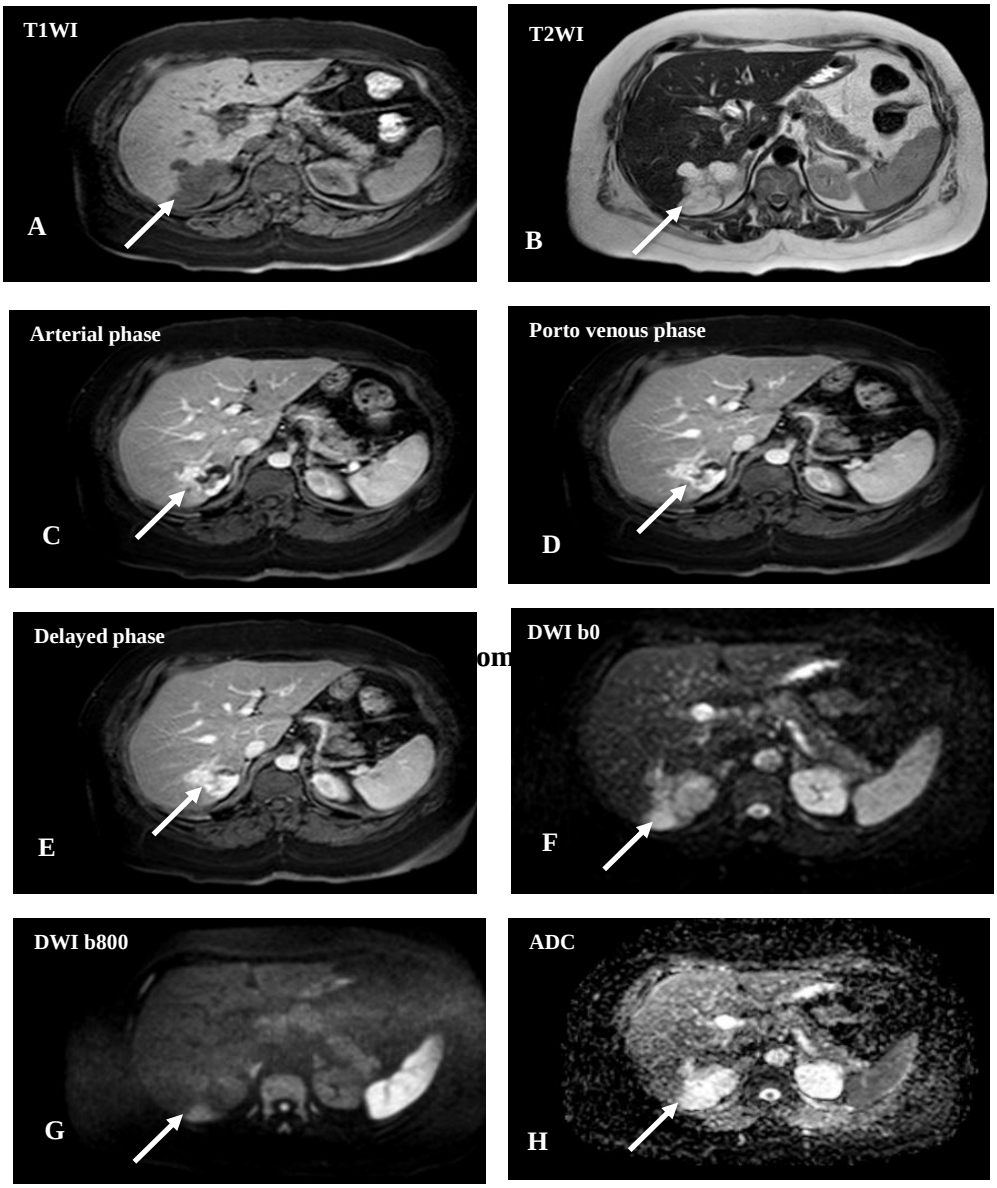

CASE 3

Clinical history: 40 years old male patient presented with history of constipation and abdominal pain. U/S was done revealed well defined cystic lesion in the right lobe of liver.

On MRI examination: the liver was of average size with a well-defined focal lesion at subsegment VI/VII measuring 47 x 41 x 53 mm in (CCxTrxAp) respectively. It elicits heterogenous intermediate signal intensity on T1WI with heterogenous high signal intensity with foci of low signal intensity and water lily sign in T2WI**(Fig. 6 A, B)** (arrows).

Dynamic MRI: the lesion elicits smooth peripheral wall enhancement **(Fig. 6 C, D, E)** (arrows)

DWI: the lesion shows decrease in signal intensity with increasing b values **(Fig. 6 F, G)** (arrows). While, it showed high signal intensity on ADC map (**Fig. 6 H)** (arrow).

ADC Value: 2.8 x $10^{-3}mm^2$/sec

MRI diagnosis: hydatid cyst

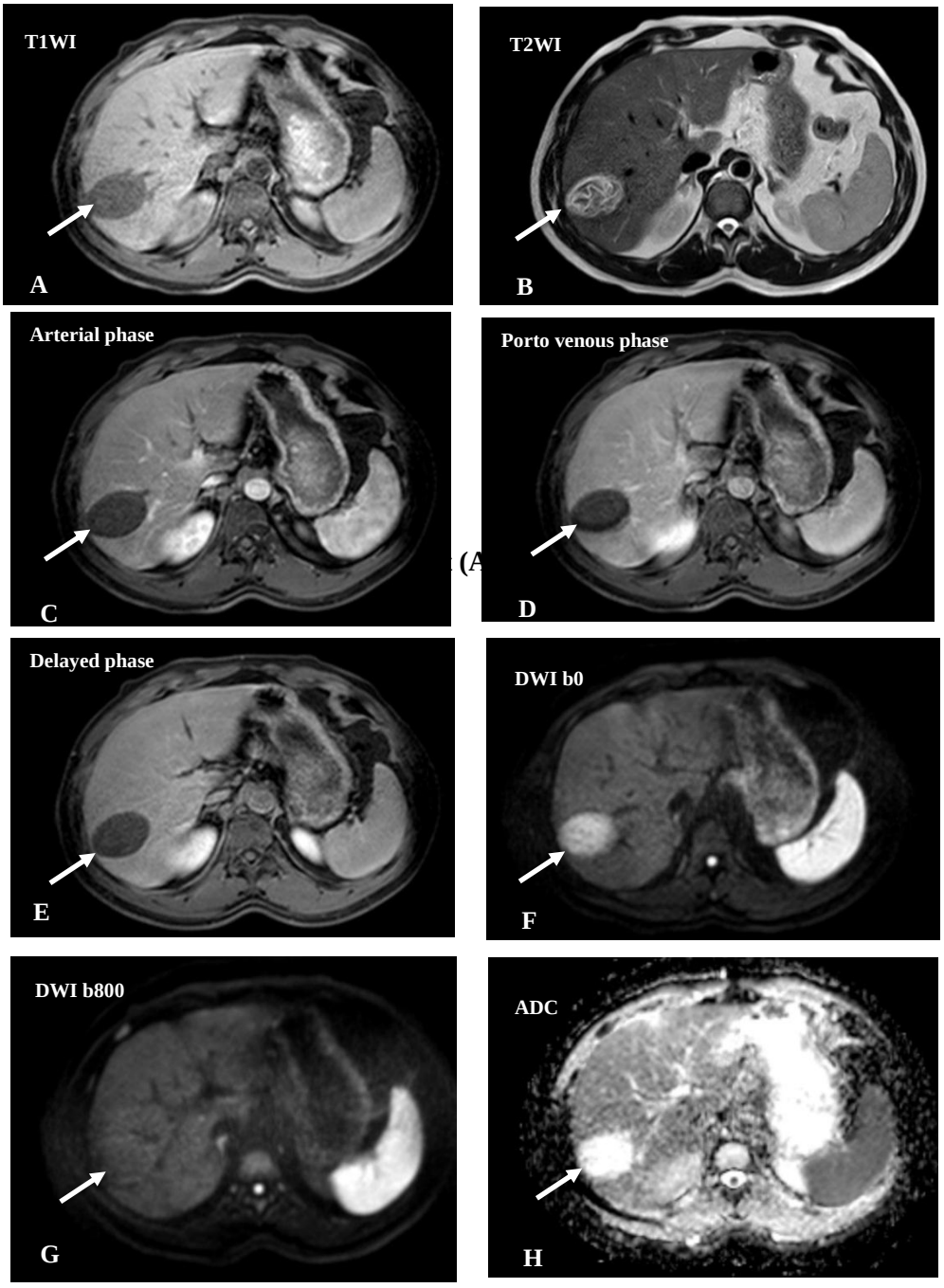

DISCUSSION

Correct detection, classification, and characterization of hepatic focal lesions are of paramount importance as they may significantly affect the choice of therapeutic approach in many cases [14]. MRI provides the most information about lesion characterization in general, and it's the most helpful in distinguishing liver lesion types and in assessing response to treatment [15].The liver is an organ in which various benign or malignant, primary or secondary masses can be detected. Today, focal masses are diagnosed using ultrasonography and/or computed tomography. Additionally, magnetic resonance imaging is preferred when further characterization of these masses is needed. MRI has many advantages (e.g., high contrast resolution, the ability to obtain images in any plane, lack of ionizing radiation, and the safety of using particulate contrast media rather than those containing iodine) that make it a favored modality [16]. The common use of dynamic enhancement studies reflected the unique vascular anatomy of the liver, which receives both arterial blood from the systemic circulation via the hepatic arteries and a larger venous blood flow from the bowel & spleen via the hepatic portal system. The importance of this dual blood supply in the investigation of hepatic diseases cannot be overstated. Some lesions, particularly those that arise from normal liver tissue, will also receive dual blood supply [17]. Although dynamic contrast enhanced examinations have become a routine component of abdominal imaging, the high cost/benefit ratio and risk of contrast media side effects remain an issue [18]. Multiphasic imaging to document the distribution of a bolus injection of contrast agent is probably the most important component of CT and MRI examinations of the abdomen, particularly for the identification and characterization of liver lesions [17]. Multiphasic MRI scanning protocols most commonly employ a multi-slice or volume spoiled gradient echo technique which allows high spatial resolution imaging of the entire region of interest during a single breath hold [17].

DW-MRI provides unique insight into tissue cellularity, tissue organization, integrity of cells and membranes, as well as the tortuosity of the extracellular space, which can be helpful for detecting malignant diseases, and for distinguishing tumour tissues from non-tumor tissues [19]. In the present study we had 7 cases of hepatic cyst, 6 cases were simple hepatic cyst (10 lesions) and 1 case was hydatid cyst (1 lesion), simple hepatic cysts they were well defined lesions, elicited hypointense signal on T1WI (28.6%) and hyperintense signal on T2WI (27.8%). This is in line with **Elsa *et al.*** [20] who reported that hepatic cysts appeared markedly hypointense on T1-WI and markedly hyperintense on T2-WI; they demonstrated no internal enhancement on contrast-enhanced images. The cyst wall was very thin or even imperceptible. They had well-defined margins and were usually oval or rounded. Using DWI, all lesions showed a decrease in signal intensity with increasing b-values and being strongly hyperintense and homogenous on ADC maps denoting benign nature. Our results showed that cyst has the highest ADC value, $3.34 \pm 0.2 \times 10^{-3}$ mm^2/sec. This is in agreement with study of **Miller *et al.*** [21] with mean ADC value $3.40 \pm 0.48 \times 10^{-3}$ mm^2/sec . Another study showed that mean of ADC value was $3.36 \pm 0.30 \times 10^{-3}$ mm^2/sec[22]. There was difference in ADC value of cyst from other study [23], with mean ADC value $2.61 \pm 0.45 \times 10^{-3}$ mm^2/sec. This variability in ADC values may be probably due to imaging parameters, b value combination or different technique either breath-hold or respiratory triggered.

Regarding hydatid cyst we had a single case with a single lesion, elicited high signal intensity with foci of low signal intensity on T2WI (2.8%) and low signal intensity in T1WI (2.9%), with post contrast capsular enhancement this is in agreement with results of **Czermak *et al.*** [24] who reported that the fluid component of the hydatid cyst was typically low on T1-weighted and high on T2- weighted images. In the presence of interluminal debris, the signal intensity became moderately inhomogeneous on both T1- and T2-weighted images. Degenerated cysts decreased in size and appeared heterogeneous, solid, or pseudo-tumor-like, whereas dead cysts were characterized by a thickened calcified wall. The fibrous capsule and internal septa appeared hypointense on T2-weighted images and showed enhancement in the post-gadolinium phase. DWI of hydatid cysts showed the same characteristics as the simple cysts [25], ADC value was 2.80×10^{-3} mm^2/sec. This in agreement with results of a previous study [26] which recorded mean ADC value $2.84 \pm 0.38 \times 10^{-3}$ mm^2/sec. In the present study we had 4 cases (4 lesions) with hepatic abscesses, lesions displayed hypointense signal intensity on T1WI (11.4%) and hyperintense signal intensity on T2WI (11.1%). On post contrast dynamic study lesions displayed peripheral ring enhancement pattern in all phases of dynamic study, this is in agreement with results of **Schneider *et al.*** [27] who explained that abscess as an area of decreased signal intensity on T1-WI and increased signal intensity on T2-WI. Perilesional edema, characterized by high signal

intensity on T2-WI, is seen in one third of cases. The abscess cavity may appear with homogeneous or heterogeneous signal intensity. Abscesses typically showed rim enhancement followed by contrast administration.

In our study, we had 2 cases (2 lesions) of adenoma, they displayed iso, hypointensity (33.3%, 2.9%) respectively on T1-WI and slight hyperintensity (5.6%) on T2WI with heterogeneous enhancement of the lesions at the arterial, portal phases of dynamic study with delayed washout. These findings agree with those of **Silva *et al.*** [28], who stated that adenomas have variable signal intensity, but can show hyperintense foci secondary to hemorrhage or intracellular lipid on T1-weighted images. Depiction of intralesional fat with fat-suppressed on opposed phase T1-weighted sequences helps distinguish adenomas from FNH. At T2-weighted imaging, these lesions have variable signal intensity but are often mildly hyperintense relative to the liver. On dynamic contrast-enhanced images, adenomas showed heterogeneous hypervascularity during the arterial phase and often demonstrates delayed contrast material washout (hypointense relative to the liver) with or without delayed-enhancing pseudocapsule. On DWI, both lesions showed slight increase in signal intensity with increasing b-values and they were hypointense on ADC maps, ADC value $1.35 \pm 0.07 \times 10^{-3}$ mm^2/sec, our results agree with those of **Agnello *et al.*** [29], with mean ADC value $1.30 \pm 0.14 \times 10^{-3}$ mm^2/sec.

In the present study we had 3 cases (3 lesions) of focal nodular hyperplasia, 2 lesions showed hypointense signal intensity (5.7%) on T1WI, hyperintense signal intensity (5.7%) on T2WI and 1 lesion displayed isointense signal intensity on both T1WI ,T2WI (33.3%, 50%) respectively. On post contrast dynamic study during the arterial phase lesions were homogeneously and strongly enhanced with the exception of the central scar, during portal phase they became isointense to the liver parenchyma and the central scar remained relatively hypointense, on delayed phase the central scar showed enhancement. These findings agree with those of **Silva *et al.*** [28], who explained that FNH is generally isointense to slightly hypointense relative to the liver on T1-weighted images and isointense to slightly hyperintense on T2-weighted images. A central scar was classically present and T1was hypointense and T2 was hyperintense because of the presence of blood vessels, bile ductules and edema within myxomatous tissue. The central scar usually showed delayed enhancement. On dynamic contrast-enhanced images, FNH showed marked, homogeneous arterial phase enhancement that became isointense during the portal venous phase. Lesions may occasionally be slightly hyperenhancing on delayed phase images. On DWI these lesions appeared generally isointense relative to adjacent liver parenchyma, ADC value $1.46 \pm 0.01 \times 10^{-3}$ mm^2/sec. Our results are similar to those of **Holzapfel *et al.*** [14], with mean ADC value $1.43 \pm 0.20 \times 10^{-3}$ mm^2/sec [30], with mean ADC value $1.49 \pm 0.04 \times 10^{-3}$ mm^2/sec. In the present study, we had 3 cases (5 lesions) of regenerative nodules, they were well-defined lesions elicited hyperintense on T1WI and appeared hypointense on T2 WI this was in line with [31], who reported that regenerating nodules without haemosiderin are typically iso to slightly hyperintense on T1-WI & iso or mildly hypointense on T2-WI.

On post contrast dynamic study lesions displayed pattern similar to the normal liver parenchyma on all phases of dynamic study this is in line with results of **Seale *et al.*** [32], who explained that most regenerative nodules enhanced to the same degree as the adjacent liver or showed slightly less enhancement. Using DWI regenerative nodule signals were similar to hepatic background, ADC value $1.22 \pm 0.1 \times 10^{-3}$ mm^2/sec.

In our result there was a significant overlap between the ADC values of adenoma, FNH and regenerative nodules with no statistically significant differences. Unfortunately, it wasn't possible to differentiate between them on basis of their ADC values nor on their appearance on DWI, however other MRI parameter can overcome this challenge. Our data was in line with those of **Miller *et al.*,** [21], where they found considerable overlap of solid benign lesions and stated that there were no statistically significant difference in ADC values between hepatic adenomas and FNH.

CONCLUSION

Benign liver lesions are frequently encountered in clinical practice and their characterization may be sometimes difficult. The problem of lesion characterization is mainly crucial and may influence therapeutic decisions and patient management. The role of imaging is therefore a mainstay and MRI, with its multi parametric potentialities, is a highly accurate method for lesion detection and characterization. Nevertheless, benign lesions may be sometimes "non typic" in their cellular content and vascular behavior and lesions biopsy can be necessary for definitive characterization.

REFERENCES

1. **Bartolozzi C (2012):** MR of the liver: from breakthrough to clinical application, Abdominal Imaging, 37(2): 154–154.
2. **Acay M, Bayramoglu S and Acay A (2014):** The sensitivity of MR colonography using dark lumen technique for detection of colonic lesions. The Turkish Journal of Gastroenterology, 25(3): 271–278.
3. **Nault J, Bioulac–Sage P, and Zucman–Rossi J (2013):** Hepatocellular benign tumors from molecular classification to personalized clinical care. Gastroenterology, 144(5): 888–902.
4. **Strassburg C and Manns M (2006):** Approaches to liver biopsy techniques revisited. Seminars in Liver Disease, 26(4): 318–327.
5. **Cogley J and Miller F (2014):** MR imaging of benign focal liver lesions. Radiologic Clinics of North America, 52(4): 657–682.
6. **Lee J (2006):** Computed Body Tomography with MRI Correlation. Lippincott Williams and Wilkins.London.pp: 312-330.
7. **Nelson R, Kamel I, Baker M *et al.* (2014):** ACR Appropriateness criteria liver lesion initial characterization. Radiology, 251(3):771-779.
8. **Ramalho M, Altun E, Herédia V*et al.* (2007):** Liver MR imaging: 1.5T versus 3T. Magnetic Resonance Imaging Clinics of North America, 15(3): 321–347.
9. **Fowler K, Brown J and Narra R. (2011):** Magnetic resonance imaging of focal liver lesions: Approach to imaging diagnosis. Hepatology, 54(6): 2227–2237.
10. **Rofsky NM, Lee VS, Laub G *et al.* (1999):** Abdominal MR Imaging with a volumetric interpolated breath-hold examination. Radiology, 212(3): 876–884.
11. **Hamm B, Thoeni R, Gould R, *et al.* (1994):** Focal liver lesions: characterization with non-enhanced and dynamic contrast material-enhanced MR imaging. Radiology, 190(2): 417–23.
12. **Galea N, Cantisani V and Taouli B (2013):** Liver lesion detection and characterization: Role of diffusion-weighted imaging. Journal of Magnetic Resonance Imaging, 37(6): 1260–1276.
13. **Koh DM and Collins DJ (2007):** Diffusion-weighted MRI in the body: applications and challenges in oncology. American Journal of Roentgenology, 188(6): 1622–1635.
14. **Holzapfel K, Bruegel M, Eiber M *et al.* (2009):** Characterization of small (</=10mm) focal liver lesions: Value of respiratory-triggered echo-planar diffusion-weighted MR imaging. European Journal Of Radiology, 25: 3161-3167.
15. **Outwater EK (2010):** Imaging of the liver for HCC. Cancer Control, 17(2):72-81.
16. **Demir O, Obuz F, Sagol O *et al.* (2015):** Contribution of diffusion-weighted MRI to the differential diagnosis of hepatic masses. Diagn. Interv. Radiol., 13: 81-86.
17. **Jackson A and Nicholson DA (2005):** Dynamic CE-MRI in the liver.In: Dynamic CE-MRI in Oncology, Springer-Verlag, Berlin Heidelberg, pp: 239-261.
18. **Hosny I (2010):** DW MRI of focal liver lesions, PJR., 20: 1-7.
19. **Thoeny HC and De Keyzer F (2007):** Extracranial applications of diffusion-weighted magnetic resonance imaging. European Radiology, 17: 1385–1393.
20. **Elsa yes KM, Narra VR, Yin Y *et al.* (2005):** Focal hepatic lesions: diagnostic value of enhancement pattern approach with contrast-enhanced 3D gradientecho MR imaging. Radiographics, 25(5):1299–320.
21. **Miller F, Hammond N, Siddiqi A *et al.* (2010)**: Utility of diffusion-weighted MRI in distinguishing benign and malignant hepatic lesions. Journal of Magnetic Resonance Imaging, 32: 138-147.
22. **Taouli B, Vilgrain V, Dumont E *et al.* (2003):** Evaluation of liver diffusion isotropy and characterization of focal hepatic lesions with two single-shot echo-planar MR imaging sequences: prospective study on 66 patients. Radiology, 226: 71-78.
23. **Koike N, Cho A, Nasu K *et al.* (2009):** Role of diffusion-weighted magnetic resonance imaging in the differential diagnosis of focal hepatic lesions. World Journal of Gastroenterology, 15: 5805-5812.
24. **Czermak B, Akhan O, Hiemetzberger R *et al.* (2008):** Echinococcosis of the liver. Abdom. Imagin., 33(2): 133-143.
25. **Kilickesmez O, Bayramoglu S, Inci E *et al.* (2009):** Value of apparent diffusion coefficient measurement for discrimination of focal benign and malignant hepatic masses. J. Med. Imaging Radiat. Oncol., 53(1):50-55.
26. **Oruc E, Yildirim N, Bolca Topal N *et al.* (2017):** Role of diffusion weighted magnetic resonance imaging (DW MRI) in classification of liver hydatid cysts and differentiation of simple cysts and abscesses from hydatid cysts. Diagnostic and Interventional Radiology, 16 (4):279–287.
27. **Schneider G, Grazioli L, Saini S *et al.* (2006):** MRI of the Liver: Imaging Techniques, Contrast Enhancement, D.D., 2nd Edition. Springer Milan, Berlin Heidelberg, New York.pp:1-40.
28. **Silva AC, Evans JM, McCullough AE *et al.* (2009):** MR imaging of hypervascular liver masses: a review of current techniques. Radiographics, 29(2):385–402.
29. **Agnello F, Ronot M, Valla D *et al.* (2012):** High-b-value diffusion-weighted MR imaging of benign hepatocellular lesions: quantitative and qualitative analysis. Radiology, 262, 511-519.
30. **Parikh T, Drew SJ, Lee VS *et al.* (2008):** Focal liver lesion detection and characterization with diffusion weighted MR imaging: comparison with standard breath-hold T2-weighted imaging. Radiology, 246: 812-822.
31. **Robert F, Diego A, Norbert K *et al.* (2008):** Cirrhosis-associated hepatocellular nodules. Radiographics, 28:747-769.
32. **Seale MK, Catalano OA, Saini S *et al.* (2009):** Hepatobiliary specific MR contrast agents: role in imaging he liver and biliary tree. Radiographics, 29(6): 1253-1277.